Contribution on the study of the all-optical processing devices and subsystems of future broadband optical networks

Adonis Bogris*
National and Kapodistrian University of Athens,
Department of Informatics and Telecommunications,
University Campus, 15784 Athens, Greece
abogris@di.uoa.gr

Abstract. In this thesis, all-optical processing for future optical networks is studied by means of parametric processes in optical fibers. Parametric processes are nonlinear effects which arise in optical fibers when high-powered waves are properly placed at specific spectral positions. The properties of parametric processes are defined by the optical fiber characteristics, the power and the wavelength position of the pump waves that are employed. In the first part of this thesis an analytical study on the noise characteristics of parametric amplifiers operating at the linear regime is provided. A useful theoretical model for the noise figure estimation is derived, and a comparative study on the noise properties of various schemes of parametric amplifiers is carried out. The second part of this thesis includes theoretical, numerical and experimental results on all-optical functionalities such as wavelength conversion, all-optical regeneration and all-optical label swapping solely based on single-pump and dual-pump parametric amplifiers. Two novel reshaping schemes accompanied by wavelength conversion are proposed and their advanced characteristics in terms of high bit-rate operation are highlighted. Finally, in the last chapter of this thesis, the potential of parametric amplification for the implementation of all-optical label swapping for photonic packet switching is proposed and numerically demonstrated for the first time up to the author's knowledge.

1 Introduction

A huge progress has been made in the recent years in optical communication systems and networks and currently, high capacity WDM point to point systems are commercially available in many configurations. As the IP traffic increases, the next step in optical network evolution will be towards all optical networking where routing and switching will be performed in the optical domain. Moreover, in the IP over fiber networking concepts, other more complicated functions as optical label erasure and re-encoding on the optical payload must be carried out in an all-optical manner. In such networking approaches, functions, as all-optical wavelength conversion and regeneration are very critical in order to deal with routing problems at the network node and to face the signal degradation due to noise accumulation by the amplifiers, jitter and dispersion.

* Assoc. Prof. Dimitris Syvridis was the supervisor of this thesis.

During the last decade, fiber-optic parametric amplifiers (FOPAs) have attracted the interest of many research groups as they are candidates for a great number of all-optical applications such as amplification, wavelength conversion, phase conjugation, 2R regeneration, return-to-zero (RZ) pulse generation, optical time-division demultiplexing, all-optical sampling and all-optical switching [1]. The above FOPA applications are mainly demonstrated using one or two high-power pump waves which are launched together with a signal in a highly nonlinear dispersion shifted fiber (HNL-DSF). The HNL-DSF's high nonlinearity along with high input power ensures a large four wave mixing (FWM) efficiency, while HNL-DSF's low dispersion slope ensures a broadband FWM efficiency. In the first part of this thesis, a theoretical study for the evaluation of the noise figure of dual-pump FOPAs, accounting for the noise characteristics of each pump source and the inherent quantum noise (QN) is presented. A comparative study between the noise characteristics of single-pump and dual-pump FOPAs is performed. In the next part of this thesis, two reshaping schemes based on FWM and parametric processes in optical fibers are proposed. On one hand, we present a simple approach for all-optical reshaping based on four-wave mixing in dispersion shifted fibers where the signal modulation is applied on the pump wave. We show that in this configuration and by proper selection of the operating conditions the obtained mixing product exhibits a significantly enhanced extinction ratio as well as improved Q factor characteristics relative to that of the modulated input wave. On the other hand, a second novel technique which takes advantage of the pump wave characteristics at the output of a single-pump fiber parametric optical amplifier (FOPA) operating under the strong pump-depletion regime is proposed. Based on the fact that the input signal intensity modulation is inversely transferred to the pump wave through the depleted parametric process, it is demonstrated that a cascade of two such FOPAs operates as an all-optical nonlinear gate with 2R (reshaping and reamplification) regenerative properties. Finally we numerically demonstrate an efficient method for the removal and insertion of DPSK modulated labels, which relies on the pump-depletion effect in fiber-optic parametric amplifiers (FOPAs). It is shown that through the depleted parametric process between the pump wave and the signal carrying the orthogonal ASK/DPSK modulation, the payload is inversely duplicated on the pump wavelength, which in advance has been phase-modulated with a new DPSK label. The proposed all-optical label swapping (AOLS) method is another all-optical signal processing application of parametric amplification, which, to the best of our knowledge, has not been addressed before.

2 Noise characteristics of fiber optic parametric amplifiers

In this section the results concerning the noise properties of FOPAs are discussed [2, 3]. First, basic theory on gain properties of dual-pump parametric amplifiers is briefly provided. Parametric amplification driven by two pump waves involves four product waves (signal and idler sidebands) that are coupled by three distinct FWM processes: modulation instability (MI), Bragg scattering (BS) and phase conjugation (PC) [4]. The PC coupling is strong in the case that two high-power pump sources are positioned at wavelengths lying on opposite sides of the zero dispersion wavelength

λ_0, relatively far apart. For signal frequencies far from each pump frequency, the MI and BS can be ignored and the parametric process is dominated by the PC FWM process for which $\omega_1+\omega_2=\omega_3+\omega_4$, where ω_j (j=1-4) are the frequencies of the two pumps, the signal, and the idler waves respectively [4, 5]. The value of the electrical noise figure of a lossless and undepleted 1P-FOPA has been analytically predicted in [6] taking into account the amplified quantum noise (AQN) and the ASE noise gathered around the pump wave. The analysis is based on the linearization of the theoretical gain expression and on the assumption of a Gaussian noise beating with the pump. The mathematical treatment of the ASE-pump and AQN-signal beatings provides the following noise figure expression, derived at the signal frequency in terms of the pump OSNR (0.1nm bandwidth):

$$NF_s = \frac{2G_s - 1}{G_s} + \frac{2P_{p-av}^2 P_s(0)\left(\frac{dG_s}{dP_p}(P_{p-av})\right)^2}{hf_s G_s \Delta f OSNR_P} \tag{1}$$

where G_s is the FOPA gain at the signal frequency f_s, $P_{p\text{-}av}$ is the average pump power, $P_s(0)$ is the input signal power, h is the Planck's constant, Δf=13GHz is the electrical filter bandwidth. In (1), the first fraction accounts for the AQN, while the second one accounts for the excess pump noise. A similar expression can be derived for the 2P-FOPA case. In this case, the gain can be described by the expression: $G_s = \frac{4\gamma^2 P_{P1} P_{P2}}{g^2}\sinh^2(gL)+1$ (P_{p1}, P_{p2} are the power values for each of the two pumps, L is the fiber length and g is the parametric gain coefficient), as long as the two pump waves are placed far apart from each other, symmetrically with respect to zero dispersion, and the input signal is not placed close to either of the two pumps to avoid the appearance of modulation instability. In this regime, the quantum-limited noise figure remains close to 3dB. Following the approach adopted for 1P-FOPAs, the noise figure for the 2P-FOPA is given by:

$$NF_s = \frac{2G_s - 1}{G_s} + \frac{2P_s(0)}{hf_s G_s \Delta f}\left[\frac{P_{p1-av}^2}{OSNR_{P1}}\left(\frac{\partial G_s}{\partial P_{p1}}(P_{p1-av}, P_{p2-av})\right)^2 + \frac{P_{p2-av}^2}{OSNR_{P2}}\left(\frac{\partial G_s}{\partial P_{p2}}(P_{p1-av}, P_{p2-av})\right)^2\right] \tag{2}$$

where $P_{pi\text{-}av}$, $OSNR_{Pi}$ (i=1, 2) is the average power and the OSNR of each pump wave. Usually, the power is the same for both pump waves. Assuming that the OSNRs are also identical, a more simplified expression can be obtained:

$$NF_s = \frac{2G_s - 1}{G_s} + \frac{4P_{p1-av}^2 P_s(0)\left(\frac{\partial G_s}{\partial P_{p1}}(P_{p1-av}, P_{p1-av})\right)^2}{hf_s G_s \Delta f OSNR_{P1}} \tag{3}$$

The noise figures for both configurations have been calculated assuming a 250m-long highly non-linear fiber with nonlinear parameter γ=12$W^{-1}Km^{-1}$, zero dispersion

wavelength λ_0=1560nm, and dispersion slope $dD/d\lambda$=0.03 ps/nm^2/km. The losses have been ignored, as they do not affect the parametric process for the short fiber length considered. For the 1P-FOPA, the pump is placed at 1561nm, while for the 2P-FOPA, the two pump wavelengths are 1530nm and 1590nm respectively, offering a flat and broadband gain profile. The peak gain for both configurations is 20dB, requiring 1W of pump power in the first configuration, and two pumps of 0.5W in the second one. The gain and the noise figure for both amplifiers are illustrated in fig. 1. The dual-pump characteristics are meaningful in the range between 1540nm-1580nm, where our theoretical approach is valid. According to fig. 1, the noise figure of 2P-FOPA is constant along the amplification bandwidth, in contrast to what is observed for the 1P-FOPA. This is somehow expected considering the gain uniformity of 2P-FOPAs. It is also observed that the noise figures of the 1P-FOPA calculated within its 3dB bandwidth (1580nm-1596nm), are higher compared to the 2P-FOPA case (bandwidth: 1540nm-1580nm), although the same OSNR is considered for the pumps of both configurations.

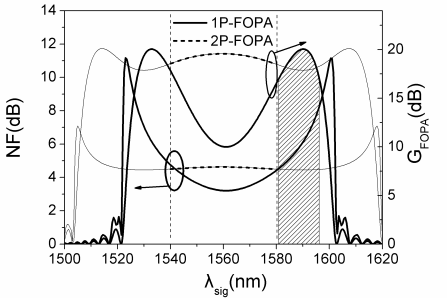

Fig.1. Gain and noise figure of 1P-FOPA and 2P-FOPA in terms of the operating bandwidth. OSNR=63dB, $P_s(0)$=-10dBm

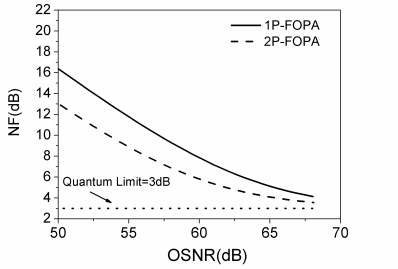

Fig.2. Noise figure of the 1P-FOPA and 2P-FOPA vs. pump OSNR. In both cases, the signal is positioned at the peak gain wavelength (1590nm and 1561nm respectively). Ps(0)=-10dBm

For example, in the gain peak of 1P-FOPA (1590nm), the noise figure is equal to 6.11dB, while for the 2P-FOPA (1561nm) the noise figure is 4.62dB. According to (1), (3), this is attributed to the quadratic dependence of the noise figure on the average pump power for constant OSNR. Considering that $P_{p1\text{-}av}=P_{p\text{-}av}/2$, higher noise figures are expected for the 1P-FOPA. Physically, it is related to the higher amount of pump noise in the case of 1P-FOPAs (OSNR=constant), which leads to a stronger pump-ASE beating at the detection. This is better illustrated in fig. 2. The difference

between the noise figures of the two schemes approaches 3dB for low OSNR values, where the dominant noise source is the excess pump noise. On the contrary, as the OSNR increases, the noise figures are approaching to each other, and the AQN determines the noise figure.

3 All-optical regeneration

In the context of this thesis, two all-optical reshaping schemes were theoretically proposed and numerically and experimentally investigated [7, 8]. Theoretical validation of the principle of operation of the first scheme is given in the next paragraph. The concept of this new idea is based on the basic FWM theory. In the rest of this work the conventional FWM notification will be used for the names of input waves, where pump and signal correspond to the higher and lower optical input respectively. As it is well known, the conjugate wave power P_C, which is produced through a FWM process, can be given by the following expression:

$$P_C(L) = \eta\gamma^2 P_P^2 P_S \exp(-\alpha L)\left\{\frac{[1-\exp(-\alpha L)]^2}{\alpha^2}\right\} \tag{4}$$

where L is the fiber length, α is the fibre attenuation coefficient, γ is the nonlinear coefficient of fibre and η represent the FWM efficiency for the conjugate wave. According to (4) the application of the modulation bit stream in the pump wave leads in conjugate wave power been proportional to the square of the pump power resulting in a corresponding extinction ratio improvement. The FWM efficiency η can be expressed as:

$$\eta = \frac{\alpha^2}{\alpha^2 + \Delta\kappa^2}\left\{1 + \frac{4\exp(-\alpha L)\sin^2(\Delta\kappa L/2)}{[1-\exp(-\alpha L)]^2}\right\} \tag{5}$$

In equation (5), Δκ is the phase-matching factor which is a function of the linear phase-matching factor $\Delta\kappa_L$ and the input wave power, due to the nonlinear refractive index change caused by the Kerr effect.

$$\Delta\kappa_L \cong \frac{\lambda_1^4}{c^2}\frac{1}{4\pi^2}\frac{dD}{d\lambda}(\omega_1-\omega_2)^2(\omega_1-\omega_0) \tag{6a}$$

$$\Delta\kappa = \Delta\kappa_L + \gamma(2P_P - P_S)\left\{\frac{1-\exp(-\alpha L_{eff})}{\alpha L_{eff}}\right\} \tag{6b}$$

According to (5), (6) the FWM efficiency η is a function of the frequency and the optical power. In the normal dispersion regime and for specific pump-signal wavelength arrangement, the converted signal power saturates at high pump power values, providing noise suppression at marks. The regenerative characteristics are more evident when two FWM modules, where the wavelength of the final regenerated output coincides to that of the input signal, in case that wavelength conversion is not preferred. The output of the first module is filtered in order to keep the conjugate output, which is then amplified and fed to the second module where it plays again the role of the pump. Together with that, a new wave is fed to the input of the second module to play the role of the signal in the FWM process and its wavelength is properly adjusted in order to achieve noise suppression at the marks. The typical

shape of such a transfer function is the so called “S shaped function”. In fig 3a typical DSF has been assumed. In fig. 3b the corresponding regenerative transfer functions are presented assuming a HNL-DSF.

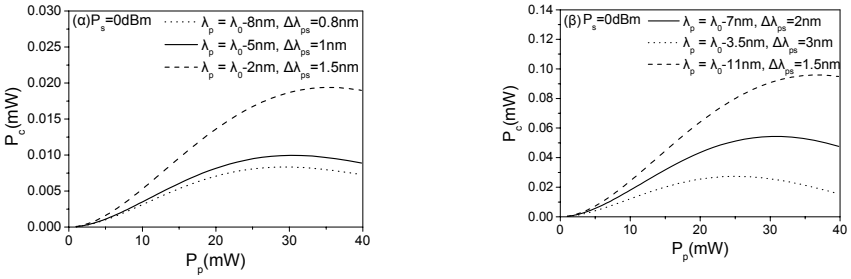

Fig. 3. Transfer functions corresponding to (a) the typical DSF and (b) the highly-nonlinear DSF for three different signal-pump wavelength spacing when (λ1-λ0) is negative. The DSF parameters are given in Table 1.

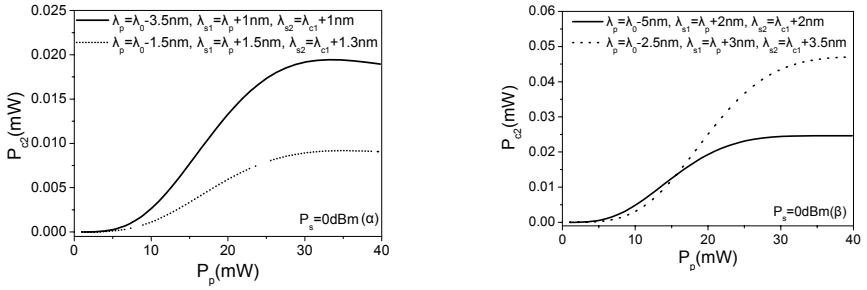

Fig. 4. Transfer functions corresponding to a two-stage wavelength converter for two different operating conditions when (a) typical DSF and (b) highly-nonlinear DSF are used respectively. The two DSF parts are considered to be identical and their parameters are given in Table 1.

In fig. 4, the transfer function of a two-stage wavelength converter is presented when typical DSF (fig. 4a) and HNL-DSF (fig. 4b) is used. In both cases, significant noise suppression characteristics have been achieved for both marks and spaces combined with extinction ratio enhancement which in some cases is almost doubled relative to the input. Numerical simulations with on-off modulated pump wave have been performed to confirm the conclusions obtained from the static transfer functions. A 256-bit NRZ sequence at 10Gb/sec is properly amplified by an EDFA including ASE noise and after being filtered by an optical bandpass filter, propagates together with a continuous wave in a DSF. In fig. 5 the output vs. input ER and Q-factor are plotted for three cases of a single stage and dual stage regenerator based on typical DSF and a dual stage regenerator based on HNL DSF. The superiority of the dual stage configuration is obvious in terms of both extinction ratio enhancement as well as Q factor improvement relative to the single stage scheme.

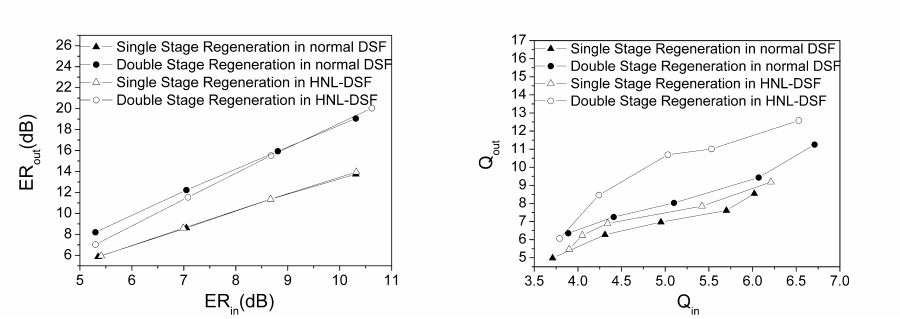

Fig. 5. Output extinction ratio and Q-factor as a function of input extinction ratio at 10Gb/sec. The operating conditions of the regenerator schemes are identical to those given in Fig. 9.

The conceptual scheme of the all-optical regenerator relying on the pump depletion effects in FOPAs is illustrated in fig. 6. An IM signal is combined with a CW pump and both are launched into the first FOPA stage. The pump1 power is initially undepleted and starts varying inversely with respect to the input signal, as signal power increases. When a certain power level is exceeded, the pump1 power starts to oscillate due to the continuously varying phase mismatch. According to fig.6(b), the noise impaired "0" bits of the input signal will be converted to the noise-free "1" bits of the pump1, as long as the "0" power does not deplete the pump. The filtered pump output of the first FOPA stage together with the CW pump2 are launched into the second FOPA stage, and as expected, the pump2 will be analogously depleted following inversely the power variations of the pump1. In that way, the pump2 carries the bit-sequence of the input signal. Through the second process, the noise is suppressed in the "0" bits of the pump1 ("1" bits of the signal). Eventually, the two cascaded FOPAs provide an IM output with suppressed power fluctuations at both marks and spaces. The regenerative characteristics of the proposed scheme are determined by the transfer function depicted in fig. 6(c). The output of the proposed regenerator lies at the pump2 wavelength, which can be selected depending on the wavelength conversion needs of the specific application.

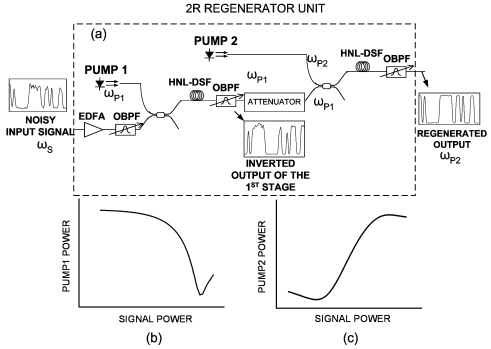

Fig.6. Setup (a) and principle of operation of the all-optical reshaping based on pump depletion effects in two cascaded FOPAs. The output pump power of the first stage is inversely dependent on the input signal (b), while the output pump of the second stage preserves the input signal shape combined with noise suppression at marks and spaces.

The performance of the all-optical reshaping scheme has been numerically evaluated for a non-return to zero (NRZ) 40-Gb/s transmission link. NLSE is numerically solved for both the transmission segments and the reshaping device. The transmission link consists of a number of similar transmission segments containing a single mode fiber (SMF), a dispersion compensating fiber (DCF), an EDFA and an OBPF having 3dB-bandwidth equal to 1nm. The Q-factor performance as a function of the transmission distance and the corresponding ER values, either with or without the utilization of the proposed regenerator, are illustrated in fig. 7.

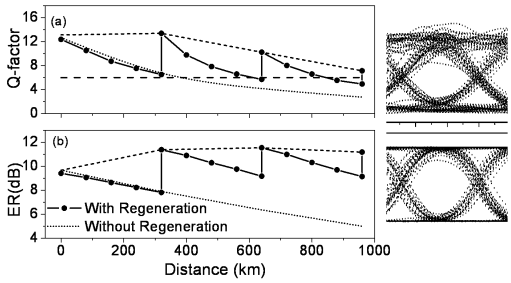

Fig.7. Q-factor (a) and extinction ratio (b) of the transmitted signal as a function of the distance. The eye diagram of the signal before (upper) and after (lower) the reshaping process are illustrated in the right side of the figure

In the former case, the reshaping device is placed every after four transmission segments which correspond to 320Km of SMF. The transmission effects degrade the Q-factor of the transmitted signal, which can be transmitted with sufficient performance up to 400Km in the case that no reshaping device is used. The employment of the reshaping device every 320Km enhances significantly the transmitted signal characteristics resulting in error-free (Q>6) performance for distances longer than 960Km.

4 All-optical label swapping

In this section a new label swapping technique which relies on the pump depletion effects in parametric amplifiers will be presented [9]. The conceptual scheme of the proposed AOLS technique is illustrated in fig. 8. Part of the ASK/DPSK modulated input is driven to the label processor for extraction of the label information and generation of the new label. The other part of the input is driven to the FOPA, where through the parametric process the two waves (pump and signal) interact providing new four-wave mixing (FWM) products. With proper adjustment of the signal power, the payload can be inversely transferred to the initially CW pump. Key point in the implementation of the proposed AOLS method is the loading of the new label on the pump wave (fig. 8). This is accomplished by utilizing a phase modulator (PM) which is also necessary for the suppression of the stimulated Brillouin scattering. It is pointed out that the output wavelength is also changed from λ_s to λ_p, thus providing two-level all-optical label swapping.

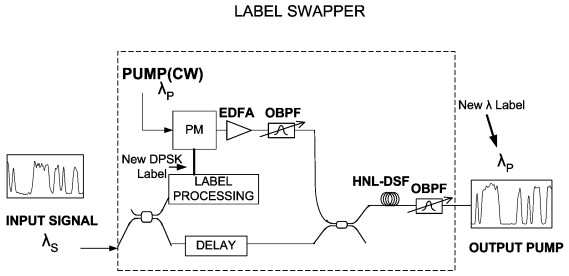

Fig.8. Schematic representation of the FOPA-based AOLS technique. HNL-DSF: Highly Non-Linear Dispersion Shifted Fiber, A: Attenuator.

The feasibility of the AOLS technique is investigated in a transmission system consisting of nodes employing the proposed swapping technique. The transmission system consists of five nodes, with the three intermediate nodes performing the proposed label swapping technique. At each node, the Q-factor of the detected payload and label is calculated after being transmitted in the fiber span. In the same figure, the Q-factor performance of both modulation formats in the case that the intermediate nodes do not perform any kind of signal processing, is also given. In the latter case the signal is transmitted over the fiber without being affected by the intermediate nodes. The Q-factor performance for both modulation formats corresponding to either of the two cases is illustrated in fig. 9. According to the figure, the payload performance degrades rapidly in terms of distance compared to the label performance. This behavior originates from the fact that the 40Gb/s payload is much more sensitive in transmission impairments than the 2.5Gb/s label. After four hops with 60Km distance and three adjacent nodes performing label swapping, the Q-factor is equal to 5.6, close to the limit of acceptable performance (Q > 6). The DPSK label quality is also impaired by the swapping process. While in the case that no intermediate swapping is performed, the label Q-factor seems to be constant over the transmission distance, in the case that the parametric swapper is utilized, its value gradually reduces, resulting in a 2 units difference at the final node.

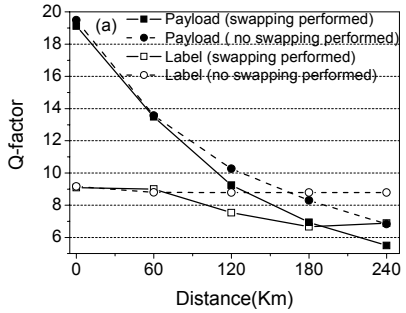

Fig.9 Q-factor performance for both payload and label in terms of transmission distance. The squares correspond to the case that the intermediate nodes perform swapping, while the circles correspond to the case that no processing is applied at the intermediate stages.

5 Conclusions

Theoretical, numerical and experimental results regarding the performance of optical amplifiers in terms of offering broadband amplification, all-optical regeneration and all-optical label swapping have been presented. A theoretical model for the estimation of the noise features of parametric amplifiers was derived. Comparison between the two basic FOPAs' schemes in terms of their noise characteristics was performed. Two reshaping schemes based solely on FWM and parametric amplification in optical fibers were numerically and in part experimentally demonstrated. These schemes are very robust in terms of the bit rate transparency (>40Gbps) and their ability of supporting both return-to zero and non-return to zero intensity modulated signals. Finally, for the first time to our knowledge, an all-optical label swapping technique based on parametric amplification was numerically tested providing promising cascadability results.

References

1. J. Hansryd, P. A. Andrekson, M. Westlund, J. Lie, and P. O. Hedekvist: Fiber-based optical parametric amplifiers and their applications, vol. 8, IEEE J. Select. Topics Quantum Electron. (2002) 506–520.
2. A. Bogris, D. Syvridis, P. Kylemark and P. A. Andrekson: Noise characteristics of dual-pump fiber-optic parametric amplifiers, vol. 23, IEEE J. Lightwave Technol. (2005), 2788-2795.
3. A. Bogris, D. Syvridis, P. Kylemark, P. Andrekson: Comparison Analysis between the Noise Properties of Single-pump and Dual-pump Fiber Optical Parametric Amplifiers, European Conference on Optical Communications 2005.
4. C. J. McKinstrie, S. Radic, and A. R. Chraplyvy: Parametric amplifiers driven by two pump waves, vol. 8, IEEE J. Selected Topics in Quantum Electron., (2002), 538-547.
5. R. H. Stolen and J. E. Bjorkholm: Parametric amplification and frequency conversion in optical fibers, vol. 18, IEEE J. Quantum Electron. (1982), 1062-1072.
6. P. Kylemark, P. O. Hedekvist, H. Sunnerud, M. Karlsson, and P. A. Andrekson: Noise characteristics of fiber optical parametric amplifiers, vol. 22, IEEE J. Lightwave Technol., (2004), 409-416.
7. A. Bogris and D. Syvridis: Regenerative Properties of a Pump-Modulated Four Wave Mixing Scheme in Dispersion Shifted Fibers, vol. 21, IEEE Journal of Lightwave Technology (2003), 1892-1902.
8. A. Bogris, H. Simos, D. Alexandropoulos, D. Syvridis: All-optical regeneration based on pump-depletion effect in fiber parametric amplification, Photonics West 2006.
9. A. Bogris, D. Syvridis: A Novel All-Optical ASK/DPSK Label Swapping Technique Based on Pump Depletion Effects in Parametric Amplifiers, submitted for publication in IEEE Journal of Lightwave Technology.